3D RF Pulses for Parallel Transmission MRI Systems

I. Graesslin[1], S. Biederer[1], P. Wilhelm[1], P. Vernickel[1], G. Mens[2], K-H. Zimmermann[3], U. Katscher[1], and P. Börnert[1]

[1]Philips Research Europe, Hamburg, Germany, [2]Philips Medical Systems, Best, Netherlands, [3]TU-Hamburg-Harburg, Hamburg, Germany

Introduction

Three-dimensional RF excitation pulses [1] have a number of interesting applications such as improved slice selective excitation, zoom imaging or spin labeling in perfusion imaging. The use of these pulses is typically limited by distortions occurring during the long pulse durations. Such effects can be overcome by the use of parallel transmission [2-4]. RF coil arrays that are segmented in three dimensions can enhance the performance and quality of 3D RF pulses by enabling pulse acceleration in up to three dimensions. This paper discusses simulations of 3D Transmit SENSE pulses using a z-segmented RF head coil as well as 3D experiments carried out on an eight-channel transmit MRI system [5] using different eight-channel transmit coils. The RF pulse calculation for parallel transmission was performed via iterative methods [6,7] exhibiting advantages in calculation time over direct matrix inversion [2-4], in particular for 3D pulses.

Methods

The calculation of 2D RF excitation pulses for parallel transmission as described in [8] was extended to 3D. The algorithm was implemented in analogy with the SENSE reconstruction [9]. The matrix inversion of the RF excitation pulse calculation was carried out iteratively using a conjugate-gradient method in the image domain. The gridding step of the non-Cartesian receive SENSE algorithm was replaced by a direct calculation of the convolution in k-space to improve the accuracy of the results.

For the iteration, the linear equation system $\mu(x')g(x') = \sum_l \left[\mu(x') S_l(x') \sum_x dPSF(x'-x)(S_l^*(x)\mu(x)\breve{g}(x)) \right]$ has to be solved for $\breve{g}(x)$ with $dPSF(x'-x) = \sum_t \frac{e^{2\pi i(x'-x)k(t)}}{D(t)}$ the density compensated point spread function, $g(x) = -i\frac{M_T(x)}{M_0}$ the normalized excitation pattern, $\mu(x)$ the intensity correction, $S_l(x)$ the coil sensitivities, l the coil index, * the conjugate complex, $D(t)$ the density correlation values, M_T the transverse magnetization, and M_0 the equilibrium magnetization. Then, the l excitation currents $I_l(t)$ are obtained by [4] $I_l(t) = \frac{1}{D(t)} \sum_x S_l^*(x)\mu(x)\breve{g}(x)\, e^{-2\pi i\, x\, k(t)}$.

Different matrix sizes N for the discretization of the field-of-excitation were used up to a resolution of N=12×12×12 pixels. For the 3D RF-pulses, a trajectory was used with a stack of 12 transverse spirals and 6 revolutions each. The corresponding gradient waveform is shown in Fig. 1. Acceleration factors up to a reduction factor of R=4 were realized by reducing the number of spiral turns resulting in a shorter gradient waveform.

Experiments were carried out on a whole body 3T MRI system (Achieva, Philips Medical Systems, The Netherlands) extended to eight parallel RF transmit channels [5].

The system was operated with a maximum gradient strength of G_{max}=31mT/m and a maximum slew rate of S_{max}=108mT/m/s. Three different eight-channel Tx/Rx RF coils were employed. A head and body coil with eight cylindrically arranged rods (angular distance 45°). Furthermore, a head coil with two subsets of four cylindrically arranged rods (angular distance 90°) and one subset of rods shifted by 45°.

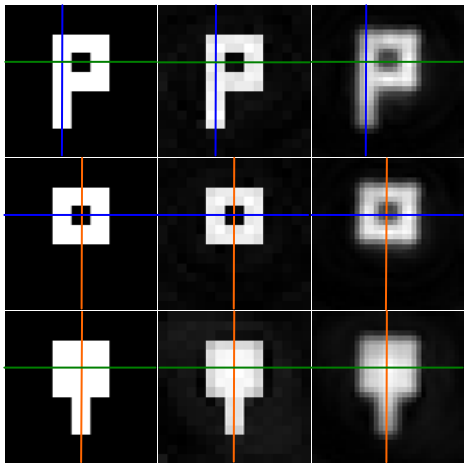

Fig. 2: Three different views of a 3D spatially selective excitation pattern. The first row shows a transverse orientation, the second row a coronal orientation, and the third row a sagittal orientation. The first column shows the demand excitation, the second column the simulated excitation, and the third column the measured excitation. The orange lines indicate transverse orientations, green coronal orientation and blue sagittal orientation.

Results and Discussion

Fig. 2 and Fig. 3 illustrate 3D RF excitations, using the integrated multi-channel body coil and a mineral oil phantom of 5 liters (diameter: 16cm, length: 37cm). Fig. 2 shows a transversal, coronal, and sagittal view of a 3D spatially selective excitation pattern. Fig. 3(a) shows an "L"-like shape desired demand excitation pattern. The corresponding simulated excitation pattern is shown in Fig. 3(b). Examples of 3D experimental results are shown for the non-accelerated pattern (Fig. 3(c)) as well as the twofold accelerated pattern (Fig. 3(d)). In the latter case, the trajectory was shortened from 6 to 4 revolutions (resulting in a pulse acceleration of 1.5). The transverse image plane corresponds to the orientation of the spirals. The Cartesian direction of the trajectory is oriented orthogonally to the image plane. The demand pattern is well reproduced for both, the non-accelerated and accelerated case. The acceleration diminishes the image quality only marginally.

Conclusion

Three-dimensional RF excitation pulses have been performed successfully on an eight-channel Tx/Rx system with and without applying parallel transmission. The use of 3D-segmented RF coils, offering RF pulse acceleration in all spatial directions, supports 3D RF pulses significantly.

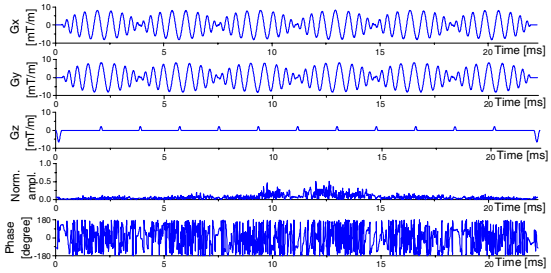

Fig. 1: Gradients for a 3D RF pulse with a reduction factor of R=1.5 and its normalized amplitude and phase.

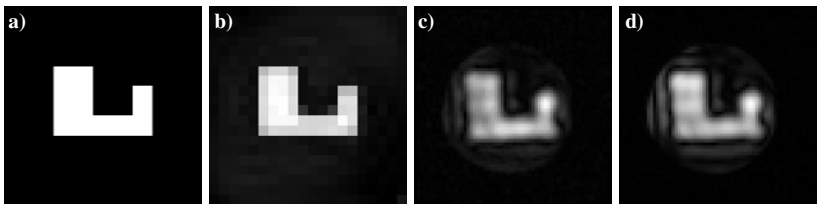

Fig. 3: Slice out of a 3D-Volume "L"-like shape target excitation pattern (a) and simulated excitation pattern (b). Examples of 3D experimental results are shown for the non-accelerated pattern (c) as well as the accelerated pattern using a reduction factor of R=2 (d).

References

[1] Pauly JM, et al. [1993] MRM 29:2-6
[2] Katscher U, et al. [2003] MRM 49:144-150
[3] Zhu Y [2004] MRM 51:775-784
[4] Grissom W, et al. [2005] ISMRM 13:19
[5] Graesslin I, et al. [2006] ISMRM 14:129
[6] Yip CY, et al. [2005] MRM 54:908-17
[7] Graesslin I, et al. [2005] MAGMA 18:S109
[8] Graesslin I, et al. [2006] ISMRM 14: 2470
[9] Pruessmann KP et al. [2001] MRM 46:638-651